

Full Length Research Paper

Synthesis of organic compounds using yellow yam (*Dioscorea praehensilis*) tyrosinase as catalyst

Olutosin Samuel Ilesanmi^{1*}, Omowumi Funke Adedugbe¹, David Adeniran Oyegoke¹,
Victory Ayo Olagunju² and Isaac Olusanjo Adewale³

¹Department of Chemical Sciences, Achievers University, Owo, Ondo State, Nigeria.

²Department of Chemistry and Biochemistry, Miami University, Oxford, Ohio, United States.

³Department of Biochemistry and Molecular Biology, Obafemi Awolowo University, Ile-Ife, Nigeria.

Received 19 May, 2023; Accepted 26 June, 2023

The authors report the synthesis of some bioactive organic compounds which could be of pharmacological interest using *Dioscorea praehensilis* tyrosinase immobilized on calcium-alginate beads. The enzymatic synthesis of these compounds involved pyruvic acid as a source of carbonyl groups, ammonia and catechol. Catechol was used as substrate and a parent compound that supplied aromatic ring carbons for the reactions. The structures of novel compounds synthesized were deduced using UV, IR and NMR spectroscopic techniques. Structural elucidation revealed that a novel lactone (3-hydroxyl-3-methylbenzo[b][1,4]-lactone) was synthesized in the presence of pyruvic acid and catechol only. When ammonia solution was introduced into the reaction system, there was conversion of the blue-colored lactone compound into a red-colored product. The structure was elucidated as 2-(2-hydroxyphenoxy)-2-aminopropanoic acid. Whereas, in the presence of ammonia and catechol only, a novel secondary amine (1,6-dihydroxy-7-aza,bicyclo[4.1.0]-2,4-heptadiene) was synthesized. Though the synthesized compounds possess functional groups, the specific pharmacological or biotechnological applications are yet to be investigated and established.

Key words: Yam Tyrosinase, catechol, novel lactone, novel amino acid, novel secondary amine.

INTRODUCTION

Tyrosinase (EC 1.14.18.1) is a copper-containing oxidoreductase, catalyzing two sequential reactions: the hydroxylation of monophenols to o-diphenols (cresolase activity), and the subsequent oxidation of o-diphenols to o-quinones (catecholase activity), both requiring molecular oxygen as the oxidizing agent (Fairhead and Thony-Meyer, 2012; Ba and Kumar, 2017), o-Quinones are highly reactive compounds that will further polymerize

non-enzymatically to form high-molecular weight brown pigments called melanin (Lai et al., 2018; Ilesanmi et al., 2022).

Tyrosinases from different species are diverse in terms of their structural properties, tissue distribution and cellular location (Mayer, 2006; Ilesanmi et al., 2023). They frequently differ with respect to their primary structure, size, and glycosylation pattern and activation

*Corresponding author. E-mail: olutosinilesanmi@yahoo.com, osilesanmi@achievers.edu.ng. Tel.: +2348062898386.

characteristics. It has been suggested that there is no common tyrosinase protein structure occurring across all species (Jaenicke and Decker, 2003). However, all tyrosinases have in common a binuclear type 3 copper centres within their active site.

Recently, the research focus on tyrosinase has moved to the biotechnological and environmental applications of the enzyme. Because of their ability to react with phenolic compounds, the enzymes have been proposed for use in a variety of biotechnological, biosensor and biocatalysts applications (Nawaz et al., 2017) such as its application in detoxification of phenol-containing wastewater and contaminant soils (Martorell et al., 2012); in food processing due to their cross-linking abilities (Ilesanmi et al., 2021); *in vitro* conjugation of the protein gelatin to the polysaccharide chitosan (Chen et al., 2002); tailoring polymers, e.g. grafting of silk proteins onto chitosan via tyrosinase reactions (Anghileri et al., 2007) and synthesis of organic chemicals (Burton, 2003; Ates et al., 2007; Valipour and Burhan, 2016). Other biotechnological applications of the enzyme include; functionalized tyrosinase-lignin nanoparticles as sustainable catalysts for the oxidation of phenols (Capecchi et al., 2018), its uses as sustainable catalysts and vehicles for the preparation of unique polyvalent bioinks (Capecchi et al., 2019), lipase-tyrosinase enzymatic cascade used in the synthesis of lipophilic hydroxytyrosol ester derivatives (Tomaino et al., 2022) and in novel amperometric biosensor based on tyrosinase/chitosan nanoparticles for sensitive and interference-free detection of total catecholamine (Gigli et al., 2022).

The use of enzymes in organic synthesis is still very much in vogue because of their stereoselectivity, specificity and eco-friendliness. It is more economical (Chapman et al., 2018). Additionally, successful organic synthesis is contingent upon product recovery from the reaction medium, enzyme's activity retention and operational stability, which could be assured by immobilization. Most molecules or compounds synthesized through traditional chemical approaches involve complicated procedures (Knowles, 2003); costly materials and metal catalysts usually under harsh conditions and offering a low conversion rate and low enantiomeric excess (Valdés et al., 2004).

Some attempts have been made for the synthetic application of tyrosinase because of its ability to convert phenolic substrates to their respective quinone derivatives. These include enzymatic biotransformation of L-tyrosine to L-DOPA using mushroom tyrosinase (Xu et al., 2012); synthesis of hydroxytyrosol, a potent antioxidant abundant in olives from tyrosol using tyrosinase (Espín et al., 2001); bioconversion of *p*-coumaric acid to caffeic acid by tyrosinase from *Pycnoporos* spp. (Halaouli et al., 2005); L-DOPA production from tyrosinase immobilized on zeolite (Seetharam and Saville, 2002) etc. In some of the

syntheses however, mixture of desired product, unreacted substrates, and the reducing agents e.g dehydroascorbic acid are obtained thus requiring further separation.

In this work, catechol was chosen as a source of aromatic ring carbon for nucleophilic attacks, to demonstrate that new compounds (lactones, secondary amine and amino acids) with pharmacological activities such as antioxidant, anti-inflammation, antifungal, anticancer, antibiotics and immunosuppressive, in addition to their use as food additives and leavening agents could be synthesized using yam tyrosinase as a biocatalyst

MATERIALS AND METHODS

Materials

Yam tuber-*Dioscorea praehensilis* was obtained from a farm around Obafemi Awolowo University, Ile-Ife campus, southwestern Nigeria. The yam cultivar was authenticated at the Ife Herbarium, Department of Botany, Obafemi Awolowo University, Ile-Ife, Nigeria.

Chemicals

All chemicals were of analytical grade and were obtained from Sigma Chemical Company, St Louis, USA, Carl Roth GmbH, Karlsruhe, Germany, or GE Healthcare Bio-sciences, Uppsala, Sweden.

Some of the equipment used include Shimadzu UV-1800 double beam spectrophotometer, Amersham Bioscience electrophoresis device, Shimadzu FTIR-8400S fourier transform-infrared spectroscopy (FT-IR) machine, Agilent ^{Unity}Inova 600 NMR spectrometer and Agilent VNMRs 300 MHz spectrometer.

Methods

Preparation of Yam Homogenates

Homogenate (30%) and crude supernatant of *D. praehensilis* were obtained according to the method described by Ilesanmi et al. (2014).

Tyrosinase activity assay

Tyrosinase activity with L-3, 4-dihydroxyphenylalanine (L-DOPA) was determined and defined according to the method of Lerch and Etlinger (1972) as modified by Ilesanmi et al. (2014).

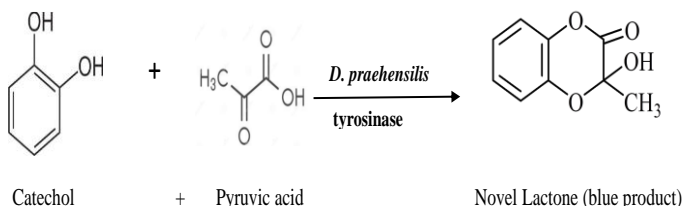
Enzyme purification and immobilization

The enzyme was purified to homogeneity using a combination of aqueous two-phase partitioning (ATPS) and size-exclusion chromatography on Sephadex G-100. Apparent homogeneity of the preparation was confirmed using SDS-PAGE (Figure 1). Pure preparations of tyrosinase from *D. praehensilis* were immobilized on calcium alginate following the method described by Ilesanmi and Adewale (2020).

Synthesis of novel organic compounds

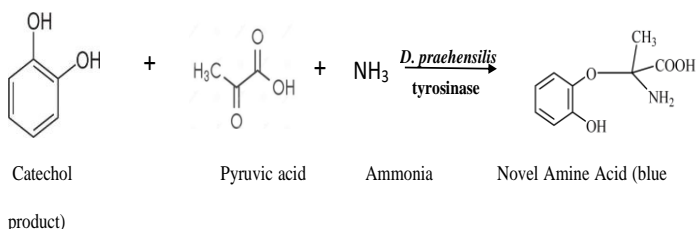
Novel Lactone: The reaction mixture consisted of catechol (1 mM) and pyruvic acid (1 mM) in 0.1 M phosphate buffer pH 6.5 and purified *D. praeheensis* tyrosinase which was immobilized on calcium-alginate beads. The beads with the reactants solution were stirred continuously for five minutes to form a blue soluble product. UV/visible absorption (200-700 nm) was measured using Shimadzu UV-1800 double beam spectrophotometer and infra-red absorption with Shimadzu FTIR-8400S machine. IR spectra values were recorded in wave number ($1/\lambda$) expressed in cm^{-1} . The spectrum was recorded over a range of 4000 - 400 cm^{-1} with a resolution of 4 cm^{-1} . The solution was thereafter lyophilized and redissolved in deuterated dimethyl sulphoxide (DMSO) for NMR spectroscopy.

Nuclear magnetic resonance (NMR): For the analysis, 100 mg of the synthesized compound was suspended in deuterated DMSO ($\text{DMSO-}d_6$). The spectra were recorded on Agilent ^{Unity}Inova 600 NMR spectrometer with a ^1H frequency of 600 MHz and a ^{13}C frequency of 150 MHz, fitted with 5mm dual channel IDPfgprobe and Agilent VNMRs 300 MHz spectrometer with a ^1H frequency of 300 MHz and a ^{13}C frequency of 75 MHz fitted with 5 mm dual channel Broadband PFG probe with chemical shift (δ) in ppm and coupling constant (J) in Hz.



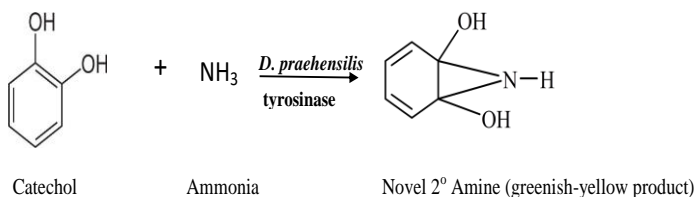
The chemical structure of the product formed was deduced using data generated from the three spectroscopic techniques.

Synthesis of novel amino acid: The same procedure as in (a) was adopted except that ammonia solution (5 mM) was introduced into the reaction mixture as a source of nitrogen.



The chemical structure was deduced in a similar manner as in (a).

Synthesis of novel secondary amine: For the synthesis of novel secondary amine, only catechol and ammonia were present in the reaction mixture. All other components remain the same.



RESULTS AND DISCUSSION

Chemical structure of the novel lactone

UV- visible spectra of the novel lactone showed a strong absorbance in the UV region with a lambda max (λ_{max}) of 277 nm, which is an indication of the presence of conjugated system of aromatic compounds (Figure 1a). A shoulder band observed between 278-280 nm in the spectrum revealed the presence of additional groups conjugated with the aromatic ring.

The IR spectrum for the synthesized compound revealed absorption bands of 3444.9, 2362.9, 1633.8, 1402.3, 1354.1, 1246.1, 1126.5, 1111.0, 1082.1, 983.7 and 719.5 cm^{-1} (Figure 1b). The absorption band in the IR spectrum at 3444.9 cm^{-1} is an indication of the presence of hydrogen-bonded O-H stretching vibrations. The bands around 2362.9 cm^{-1} are ascribed to the presence of sp^2 hybridized C-H stretching. Absorption signal at 1633.8 cm^{-1} revealed the presence of conjugated C=O and sp^2 hybridized carbon (C=C) of aromatic rings. The spectra region from 1402.3-1246.1 cm^{-1} confirms the presence of aromatic ring. Absorption peak at 1126 cm^{-1} shows the presence of C-O stretching of aromatic cyclic esters. Out-of-plane signal at 719.5 cm^{-1} is typical of ortho-disubstituted benzene ring.

In the NMR spectra (Figure 1c), the following data assignments were obtained: ^1H NMR (300 MHz, $\text{DMSO-}d_6$) δ 8.12 (d, $J = 1.4$ Hz, 1H), 7.56 (d, $J = 1.4$ Hz, 1H), 7.43 – 7.16 (m, 1H), 7.01 – 6.66 (m, 1H), 3.65 (s, 2H), 2.76 – 2.52 (m, 1H), 2.49 – 2.33 (m, 1H), 2.33 – 2.21 (m, 1H), 2.27 – 2.01 (m, 1H), 2.05 – 1.83 (m, 2H), 1.84 (d, $J = 5.7$ Hz, 1H), 1.83 – 1.56 (m, 2H), 1.48 – 1.33 (m, 1H), 1.38 – 1.22 (m, 1H), 1.27 (s, 1H), 1.27 – 1.08 (m, 4H), 1.14 – 0.81 (m, 1H). The ^{13}C NMR data obtained are: (75 MHz, $\text{DMSO-}d_6$) δ 172.75, 169.28, 168.64, 156.89, 148.39, 123.81, 121.20, 72.73, 70.20, 60.63, 47.77, 24.30, 23.20. ^1H NMR spectra revealed the presence of four (4) aromatic proton signals at 7.38, 7.24, 6.89 and 6.08 ppm which appear as doublet of doublets and doublet of multiplets. It also showed signal at 1.87 ppm which is typical of sp^3 hybridized methyl group as a singlet and at 2.29 ppm, typical of hydroxyl group as a result of proton unexchanged with deuterium. Signals 8.41, 8.12 and 7.55 ppm may be due to the unreacted diols in the reaction mixture. ^{13}C NMR spectra revealed nine (9) non-equivalent carbon signals at 173, 168, 167, 148, 144, 131, 123, 120 and 23 ppm present in the compound (Figure 1d). Signal 173 ppm is due to presence of carbonyl (C=O) stretching of cyclic esters. Signals 168 and 167 ppm are ascribed to the two oxygenated carbon present in the compound while the signals at 148, 144, 131 and 123 ppm is typical of the four aromatic carbon atoms in the benzene ring of the compound. The chemical shift of 120 ppm is an indication of sp^3 hybridized carbon. The absorption frequency is

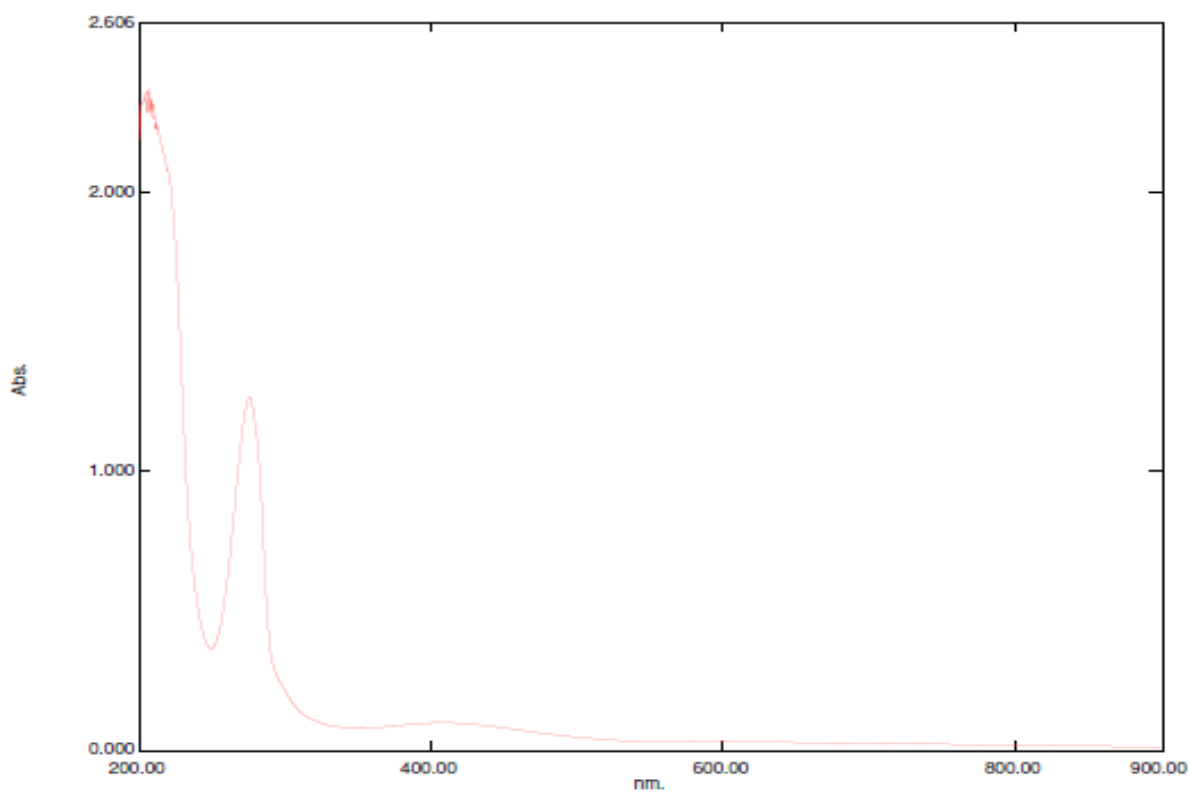


Figure 1a. Ultraviolet spectrum of novel lactone.
Source: Authors

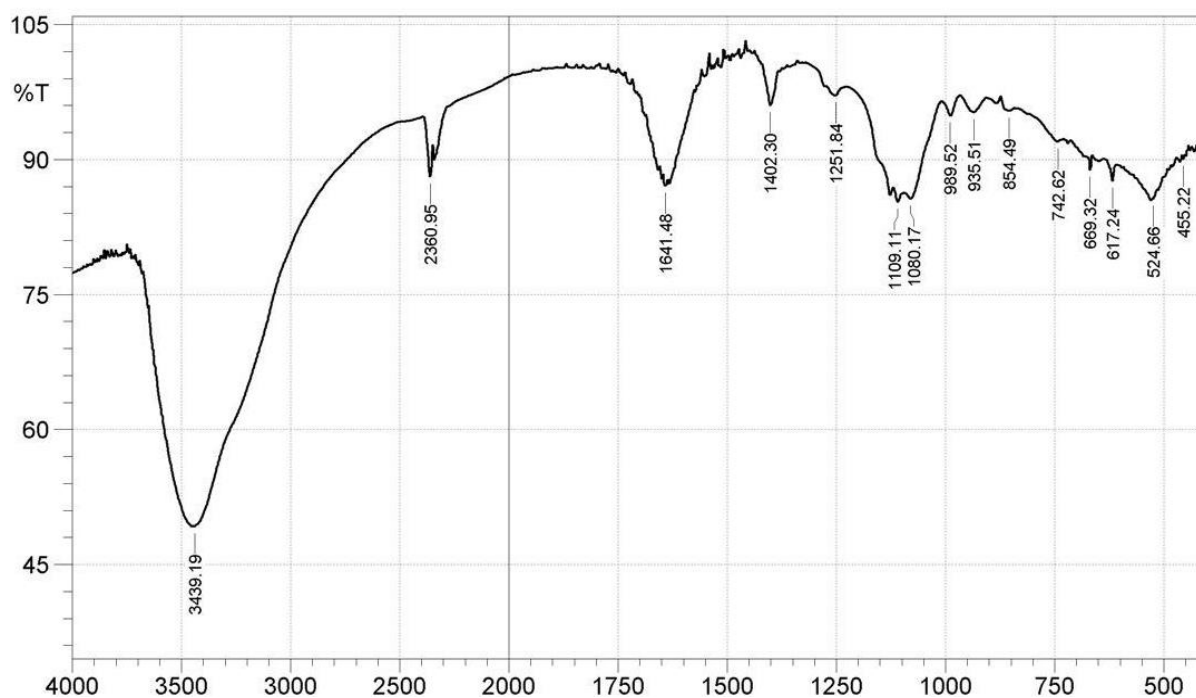


Figure 1b. Infrared spectrum of novel lactone.
Source: Authors

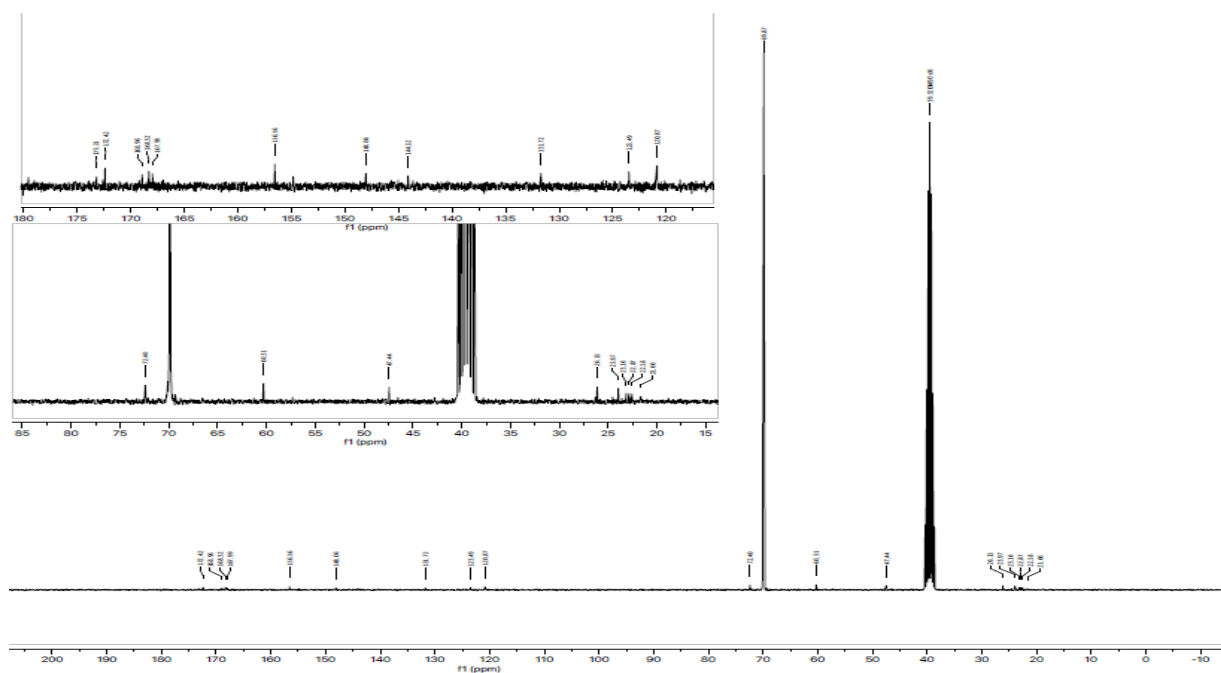


Figure 1d. ^{13}C NMR Spectra of the novel lactone.
Source: Authors

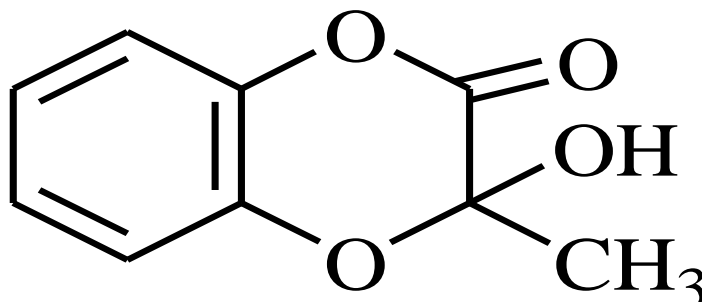


Figure 1e. Chemical structure of the novel lactone (3-hydroxyl-3-methylbenzo[b][1,4]-lactone) (*Sanjone*).
Source: Authors

3.80 - 3.69 (m, 14H), 3.35 (d, $J = 5.1$ Hz, 1H), 3.34 - 3.23 (m, 15H), 3.23 - 3.15 (m, 2H), 3.19 - 3.07 (m, 6H), 3.05 (s, 1H), 2.93 (d, $J = 23.9$ Hz, 4H), 2.61 - 2.52 (m, 5H), 2.52 - 2.40 (m, 7H), 2.40 - 2.30 (m, 4H), 2.17 (s, 1H), 1.91 (s, 2H), 1.62 (s, 1H), 1.54 (s, 1H), 1.48 (s, 4H), 1.35 (d, $J = 7.3$ Hz, 1H), 1.31 - 1.06 (m, 33H), 0.92 - 0.79 (m, 6H). The ^1H NMR spectra of the amine show four (4) aromatic proton signals at 7.70, 6.96, 6.69 and 6.57 ppm. It also revealed signals at 4.13 ppm which is typical of the presence of NH group and at 2.96 ppm, typical of hydroxyl (OH) group.

On the basis of these analysis, the structure of the novel secondary amine was deduced to be 1,6-

dihydroxy-7-aza,bicyclo[4.1.0]-2,4-heptadiene (Figure 2d). For ease of reference, this compound was called *Tosamine*. Generally, secondary amines are potent physiologically active compounds (Insaf and Witiak, 1999). The newly synthesized compound may therefore have various pharmacological applications (Holmes et al., 2013).

Chemical structure of the novel amino acid

UV- visible spectra of the compound revealed a strong absorbance in the UV region with a lambda max (λ_{max}) of

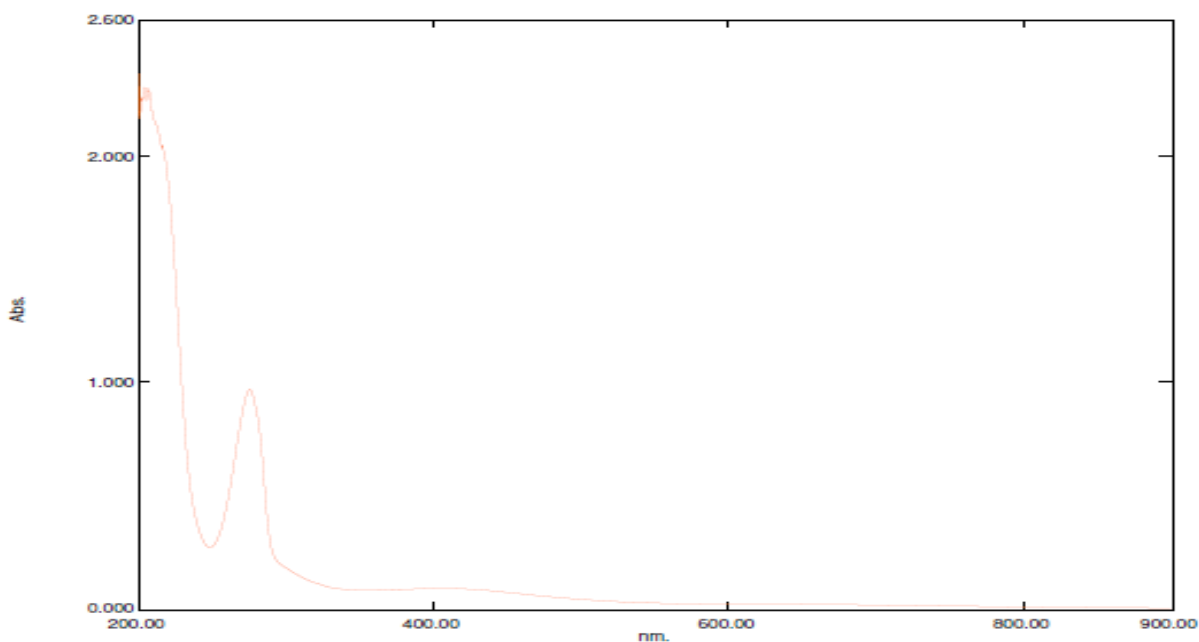


Figure 2a. UV Spectrum of the novel secondary amine.
Source: Authors

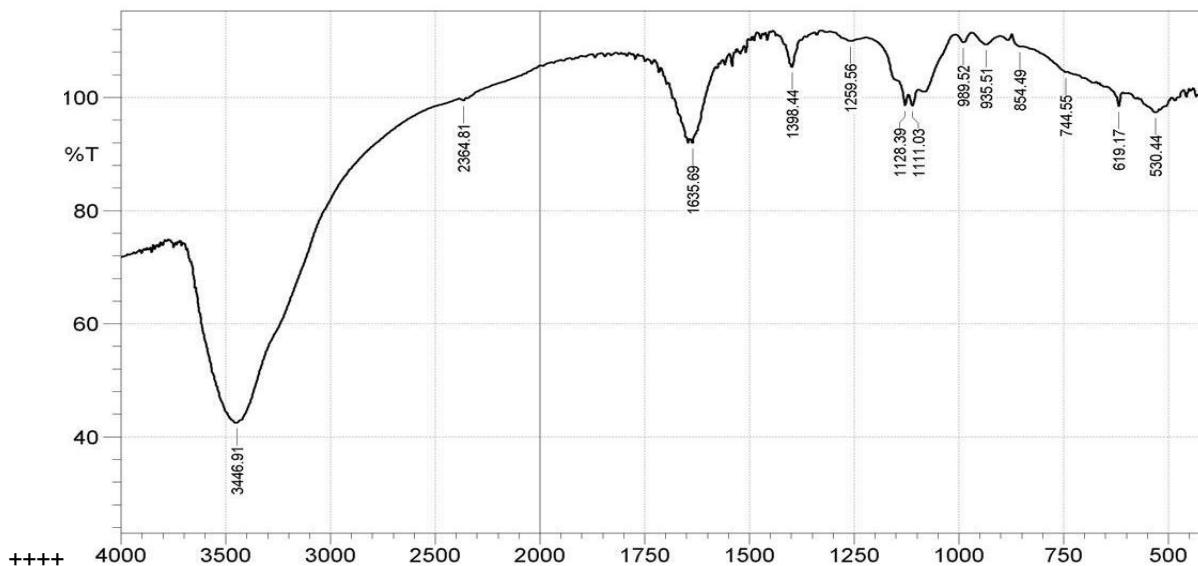


Figure 2b. The infrared spectrum of the novel secondary amine.
Source: Authors

277 nm, typical of the presence of conjugated double bond system of aromatic compounds (Figure 3a). A shoulder band observed between 278-280 nm in the spectrum revealed the presence of additional group conjugated with the aromatic ring. The absorption bands obtained from the IR spectrum were 3443.1, 2345.5,

1631.8, 1400.4, 1356.0, 1249.9, 1161.2, 1124.5, 1109.1, 1080.2, 987.6, 939.4 and 617.2 cm^{-1} (Figure 3b). The absorption band at 3443.1 cm^{-1} is due to the presence of hydrogen-bonded O-H stretching and NH_2 stretching of aromatic primary amine, although it is not appearing as two peaks. The bands around 2345.5 cm^{-1} revealed the

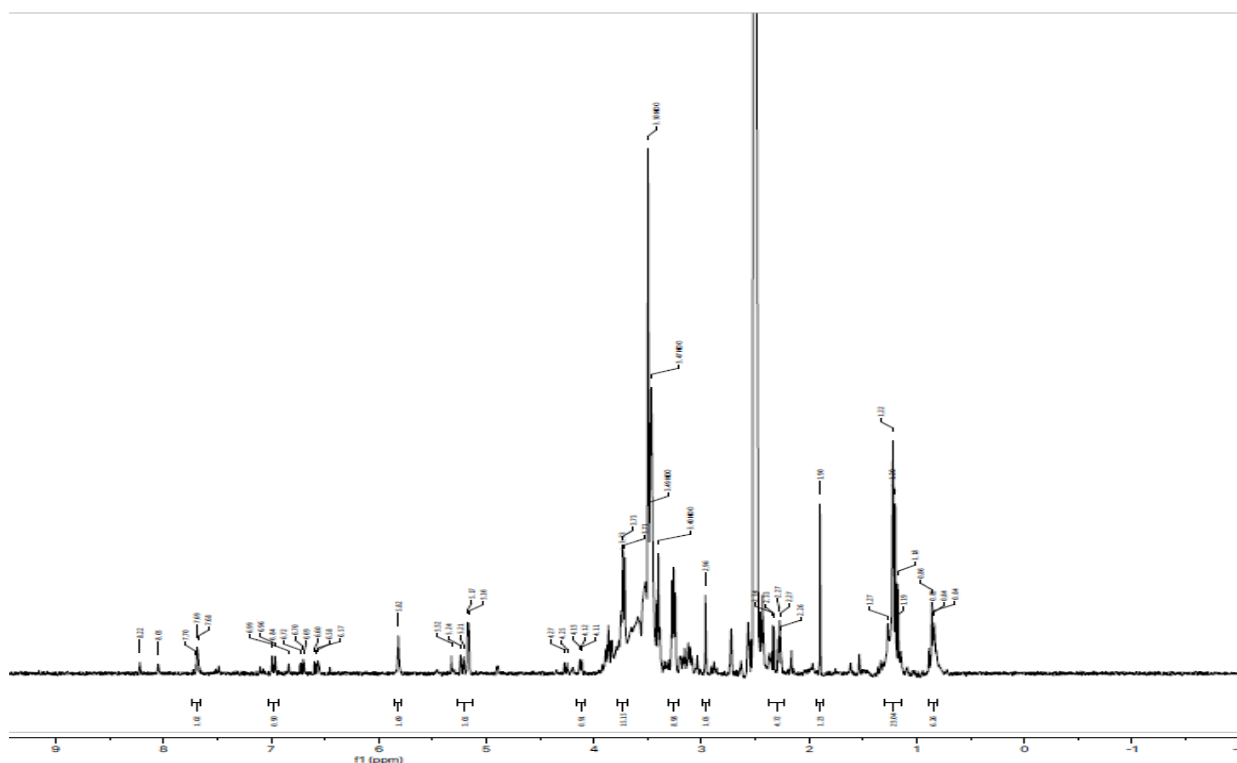


Figure 2c. ^1H NMR spectra of the novel amine.
Source: Authors

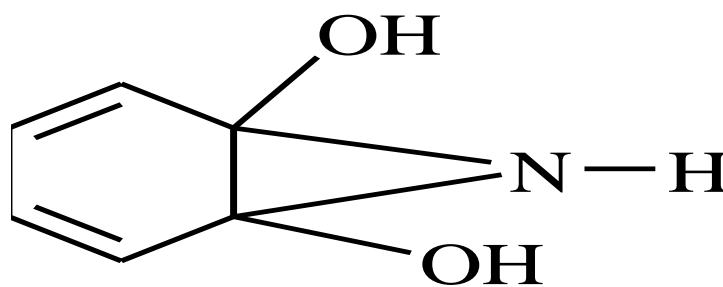


Figure 2d. Chemical structure of the novel secondary amine (1,6-dihydroxy-7-aza,bicyclo[4.1.0]-2,4-heptadiene) (*Tosamine*).
Source: Authors

presence of sp^2 hybridized C-H stretching. Absorption signal at 1631.8 cm^{-1} is typical of the presence of carbonyl group (C=O) stretching of carboxylic acid and sp^2 hybridized carbon (C=C) of aromatic rings. The spectra region from $1400.4\text{--}1249.9\text{ cm}^{-1}$ indicates the presence of aromatic ring. Whereas absorption peaks at region between $1161.2\text{--}1080.2\text{ cm}^{-1}$ is due to the presence of C-O stretching of aromatic cyclic esters. The absorption bands at region between $987.6\text{--}617.24\text{ cm}^{-1}$ are the fingerprint region which may be of no diagnostic value.

In the NMR spectra, the following data assignments were obtained (Figure 3c): ^1H NMR (300 MHz, DMSO-d_6) δ 8.11 (s, 1H), 7.59 – 7.46 (m, 2H), 7.44 (s, 1H), 7.44 – 7.30 (m, 2H), 7.30 – 6.99 (m, 1H), 6.90 – 6.71 (m, 2H), 6.69 (s, 1H), 6.75 – 6.54 (m, 1H), 6.07 (q, $J = 1.5$ Hz, 0H), 5.86 – 5.70 (m, 1H), 5.34 – 5.14 (m, 1H), 3.73 (dd, $J = 5.7, 3.9$ Hz, 1H), 3.34 – 3.22 (m, 1H), 2.67 – 2.53 (m, 1H), 2.48 – 2.32 (m, 3H), 2.37 – 2.15 (m, 2H), 2.20 – 2.03 (m, 1H), 2.08 – 1.89 (m, 1H), 1.94 – 1.73 (m, 9H), 1.58 (dd, $J = 20.1, 3.0$ Hz, 1H), 1.51 – 1.29 (m, 3H), 1.23 (s, 16H), 1.34 – 1.13 (m, 14H), 1.14 (d, $J = 4.0$ Hz, 1H), 1.11

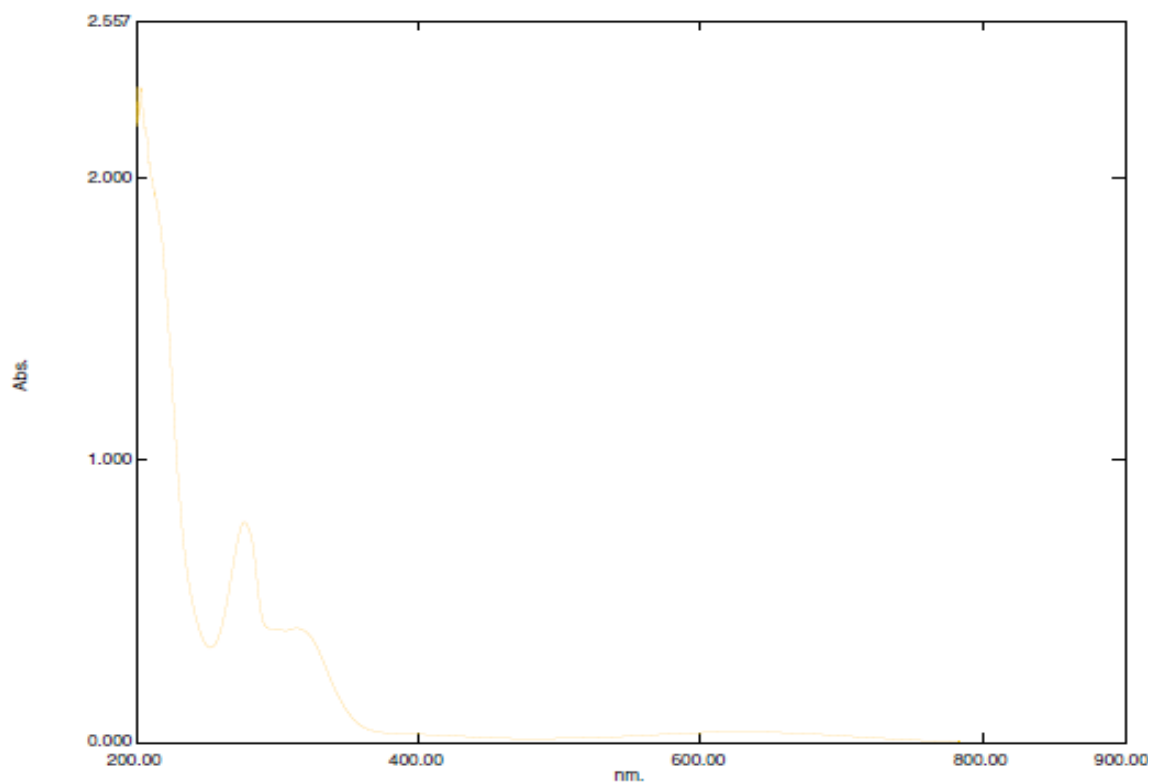


Figure 3a. UV spectrum of the novel amino acid.
Source: Authors

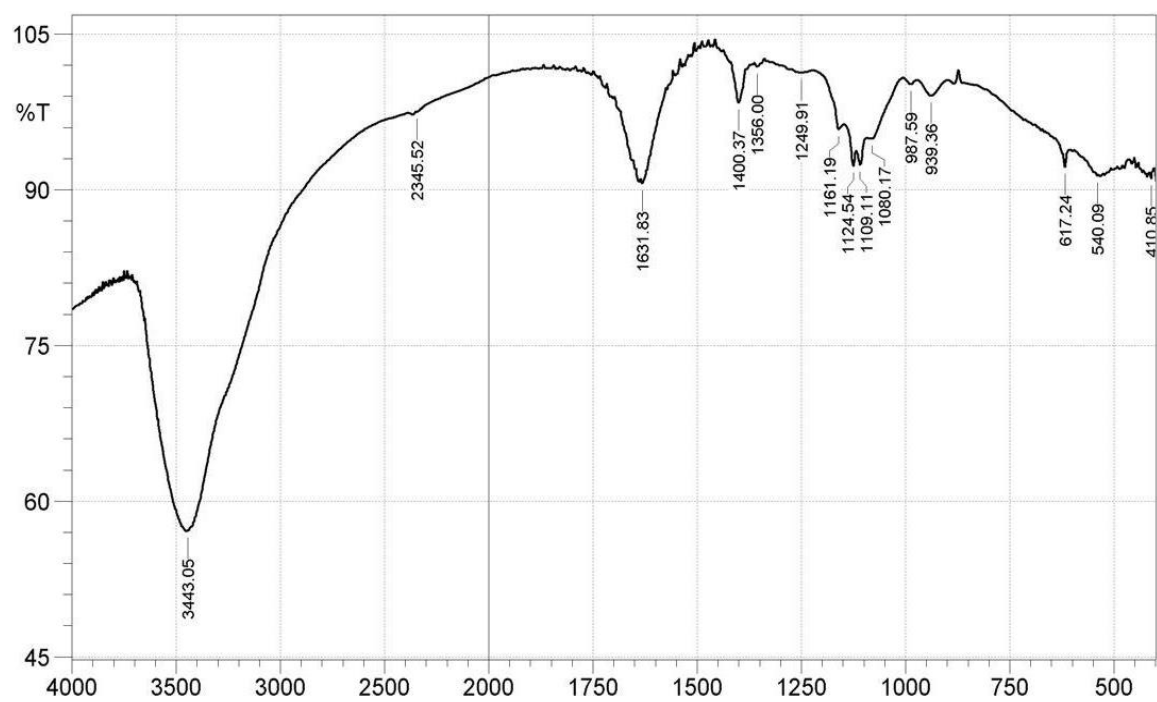


Figure 3b. The infrared spectrum of the novel amino acid.
Source: Authors

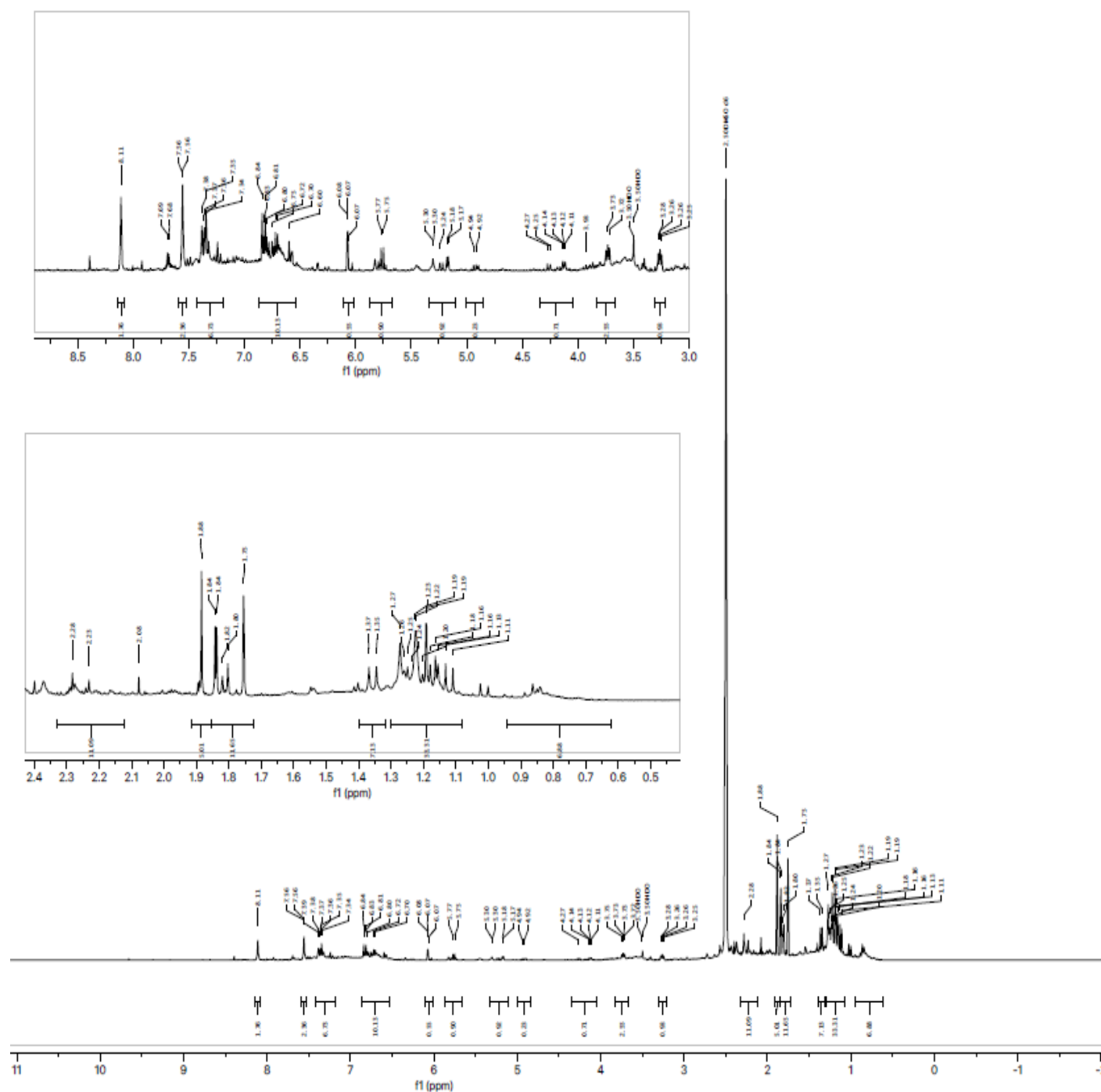


Figure 3c. ^1H NMR spectra of the novel amino acid.
Source: Authors

(s, 1H), 1.09 – 0.90 (m, 1H), 0.94 – 0.81 (m, 1H), 0.87 – 0.69 (m, 1H). The ^1H NMR spectra of the novel amino acid revealed seven signals of diagnostic value. Four signals at 7.18, 6.84, 6.72 and 6.08 ppm are typical of aromatic protons. Also, a signal with a chemical shift of

2.28 ppm which appears as singlet, is an indication of the presence of methyl group (CH_3), a sp^3 hybridized carbon. It also revealed another signal with a shift of 3.28 ppm, which is due to the presence of NH_2 group. A signal with a shift of 3.08 ppm is ascribed to hydroxyl (OH) group of

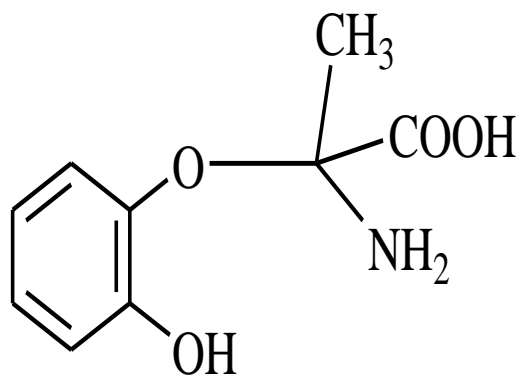


Figure 3d. Chemical structure of the novel amino acid (2-(2-hydroxyphenoxy)-2-aminopropanoic acid (*Laitane*)).

Source: Authors

aromatic carboxylic acid. The reduction in the chemical shift of the hydroxyl group upfield could be as a result of acidic-labile proton. The structure of the novel amino acid was deduced to be 2-(2-hydroxyphenoxy)-2-amino propanoic acid (Figure 3d). For ease of reference, this compound was called *Laitane*. Some aromatic amino acids such as phenylalanine, tyrosine and tryptophan are precursors of neurotransmitters (the catecholamines); as an antidepressant and in the control of mood (Young, 2013). The synthesized amino acid may probably perform similar function due to similarities in their structures. The presence of carboxylic group, amino group and hydroxyl group in the structure of the compound could be exploited for other pharmacological or biotechnological applications.

CONFLICT OF INTERESTS

The authors have not declared any conflict of interests.

REFERENCES

- Anghileri A, Lantto R, Kruus K, Arosio C, Freddi G (2007). Tyrosinase-catalyzed grafting of sericin peptides onto chitosan and production of protein-polysaccharide bioconjugates. *Journal of Biotechnology* 127:508-519.
- Ates S, Cortenlioglu E, Bayraktar E, Mehmetoglu U (2007). Production of L-DOPA using Cu-alginate gel immobilized tyrosinase in a batch and packed bed reactor. *Enzyme and Microbial Technology* 40:683-687.
- Ba S, Kumar VV (2017). Recent developments in the use of tyrosinase and laccase in environmental applications. *Critical Reviews in Biotechnology* doi: 10.1080/07388551.2016.1261081.
- Burton SG (2003). Laccases and phenol oxidases in organic synthesis – a review. *Current Organic Chemistry* 7:1317-1331.
- Capecchi E, Piccinino D, Bizzarri BM, Avitabile D, Pelosi C, Colantonio C, Calabrò G, Saladino R (2019). Enzyme-lignin nanocapsules are sustainable catalysts and vehicles for the preparation of unique polyvalent bioinks. *Biomacromolecules* 20(5):1975-1988.
- Capecchi E, Piccinino D, Delfino I, Bollella P, Antiochia R, Saladino R (2018). Functionalized tyrosinase-lignin nanoparticles as sustainable catalysts for the oxidation of phenols. *Nanomaterials* 8:438.
- Chapman J, Ismail AE, Dinu CZ (2018). Industrial applications of enzymes: Recent advances, techniques, and outlooks. *Catalysts* 8:238.
- Chen T, Embree HD, Wu LQ, Payne GF (2002). In vitro protein-polysaccharide conjugation: tyrosinase-catalyzed conjugation of gelatin and chitosan. *Biopolymers* 64(6):292-302.
- Espín JC, Soler-Rivas C, Cantos E, Tomas-Barberan FA, Wichers HJ (2001). Synthesis of the antioxidant hydroxytyrosol using tyrosinase as biocatalyst. *Journal of Agriculture and Food Chemistry* 49(3):1187-1193.
- Fairhead M, Thöny-Meyer L (2012). Bacterial tyrosinases: old enzymes with new relevance to biotechnology. *New Biotechnology* 29(2):183-191.
- Gigli V, Tortolini C, Capecchi E, Angeloni A, Lenzi A, Antiochia R (2022). Novel amperometric biosensor based on tyrosinase/chitosan nanoparticles for sensitive and interference-free detection of total catecholamine. *Biosensors* 12:519.
- Halaouli S, Asther MI, Kruus K, Guo L, Hamdi M, Sigoillot JC, Asther M, Lomascolo A (2005). Characterization of a new tyrosinase from *Pycnoporus* species with high potential for food technological applications. *Journal of Applied Microbiology* 98(2):332-343.
- Holmes A, Christelis N, Arnold C (2013). Depression and chronic pain. *The Medical Journal of Australia* 199:S17-S20.
- Hur J, Jang J, Sim J (2021). A review of the pharmacological activities and recent synthetic advances of γ -Butyrolactones. *International Journal Molecular Science* 22(5):2769.
- Ilesanmi OS, Adedugbe OF, Adewale IO (2021). Potentials of purified tyrosinase from yam (*Dioscorea* spp) as a biocatalyst in the synthesis of cross-linked protein networks. *Heliyon* 7:e07831
- Ilesanmi OS, Adedugbe OF, Oyegoke DA (2022). Some physicochemical properties of tyrosinase from sweet potato (*Ipomea batatas*). *African Journal of Biotechnology* 21(12):553-558.
- Ilesanmi OS, Adedugbe OF, Oyegoke DA, Adebayo RF, Agboola OE (2023). Biochemical properties of purified polyphenol oxidase from bitter leaf (*Vernonia amygdalina*). *Heliyon* 9:e17365
- Ilesanmi OS, Adewale IO (2020). Physicochemical properties of free and immobilized tyrosinase from different species of yam (*Dioscorea* spp). *Biotechnology Reports* e00499.
- Ilesanmi OS, Ojopagogo YA, Adewale IO (2014). Kinetic characteristics of purified tyrosinase from different species of *Dioscorea* (Yam) in aqueous and non-aqueous systems. *Journal of Molecular Catalysis B: Enzymatic* 108:111-117.
- Insaf SS, Witiak DT (1999). Facile non-racemizing route for the *N*-alkylation of hindered secondary amines. *Synthesis* 3:435-440.
- Jaenicke E, Decker H (2003). Tyrosinases from crustaceans form hexamers. *Biochemical Journal* 371(2):515-523.
- Knowles WS (2003). Asymmetric hydrogenations. *European Journal of Organic Chemistry* 345:3-13.
- Lai X, Wichers HJ, Soler-Lopez M, Dijkstra BW (2018). Structure and function of human tyrosinase and tyrosinase-related proteins. *Chemistry: A European Journal* 24(1):47-55.
- Lerch K, Etlinger L (1972). Purification and characterization of a tyrosinase from *Streptomyces glaucescens*. *European Journal of Biochemistry* 31(3):427-437.
- Lindsay RM, Smith W, Lee WK, Dominiczak MH, Baird JD (1997). The effect of delta-gluconolactone, an oxidised analogue of glucose, on the nonenzymatic glycation of human and rat haemoglobin. *Clinica Chimica Acta* 263(2):239-247.
- Martin F, Cayot N, Marin A, Journaux L, Cayot P, Gervais P, Cachon R (2009). Effect of oxidoreduction potential and of gas bubbling on rheological properties and microstructure of acid skim milk gels acidified with glucono-delta-lactone. *Journal of Dairy Science* 92(12):5898-5906.
- Martorell MM, Pajot HF, Rovati JI, Figueroa LIC (2012). Optimization of culture medium composition for manganese peroxidase and tyrosinase production during Reactive Black 5 decolourization by the yeast *Trichosporon akiyoshidainum*. *Yeast* 29(3-4):137-144.
- Mayer AM (2006). Polyphenol oxidases in plants and fungi: going

- places? A review. *Phytochemistry* 67(21):2318-2331.
- Nawaz A, Shafi T, Khaliq A, Mukhtar H, ul Haq I (2017). Tyrosinase: Sources, Structure and Applications. *International Journal of Biotechnology and Bioengineering* 3(5):142-148.
- Seetharam G, Saville BA (2002). L-DOPA production from tyrosinase immobilized on zeolite. *Enzyme and Microbial Technology* 31(6):747-753.
- Tomaino E, Capecchi E, Piccinino D, Saladino R (2022). Lignin nanoparticles support lipase-tyrosinase enzymatic cascade in the synthesis of lipophilic hydroxytyrosol ester derivatives. *Chemcatchem* 14(18):00380.
- Valdés RH, Puzer L, Gomes M, Marques CESJ, Aranda DAG, Bastos ML, Gemal A, Antunes OAC (2004). Production of L-DOPA under heterogeneous asymmetric catalysis. *Catalysis Communication* 5(10):631-634.
- Valipour E, Burhan A (2016). Increased production of tyrosinase from *Bacillus megaterium* strain M36 by the response surface method. *Archives of Biological Sciences* 68(3):659-668.
- Xu DY, Chen JY, Yang Z (2012). Use of cross-linked tyrosinase aggregates as catalyst for synthesis of L-DOPA. *Biochemical Engineering Journal* 63:88-94.
- Young SN (2013). Acute tryptophan depletion in humans: A review of theoretical, practical and ethical aspects. *Journal of Psychiatry and Neuroscience* 38(5):294-305.